https://doi.org/10.5194/egusphere-2024-1736
Preprint. Discussion started: 18 July 2024

Hemispheric asymmetry in recent stratospheric age of air changes

Kimberlee Dubé[1], Susann Tegtmeier[1], Felix Ploeger[2], and Kaley A. Walker[3]

[1]Institute of Space and Atmospheric Studies, University of Saskatchewan, Saskatoon, SK, Canada
[2]Forschungszentrum Jülich, Jülich, Germany
[3]Department of Physics, University of Toronto, Toronto, ON, Canada

Correspondence: Kimberlee Dubé (kimberlee.dube@usask.ca)

Abstract. Many stratospheric trace gases, including O_3, HCl, and NO_y, have opposing trends in the Southern Hemisphere (SH) compared to the Northern Hemisphere (NH) during the last two decades. Some of this difference is due to hemispherically asymmetric changes in the rate of transport by the Brewer-Dobson Circulation (BDC), and some is due to ozone depletion and recovery. The mean Age of Air (AoA) is a common proxy for the transport rate by the BDC in models, however it cannot be directly measured. We use observations from the Atmospheric Chemistry Experiment Fourier Transform Spectrometer (ACE-FTS) along with results from the Chemical Lagrangian Model of the Stratosphere (CLaMS) to derive AoA anomalies and AoA trends. The AoA is derived using observations of N_2O, CH_4, and $CFC-12$, all long-lived trace gases with tropospheric sources. We also consider CLaMS simulations driven with four different reanalyses (ERA5, ERA-Interim, JRA-55, MERRA-2). We find that, irrespective of which trace gas or reanalysis is used, air in the NH aged by up to 0.3 years/decade relative to the SH over 2004–2017. The maximum hemispheric difference in aging occurs in the middle stratosphere, near 30 hPa (∼24 km). We also show that the aging rate in the NH becomes smaller when the analysis is extended to 2021. The observed aging in the NH middle stratosphere contradicts model predictions of a decrease in stratospheric AoA in response to rising atmospheric greenhouse gas levels. However, the smaller aging rate during 2004–2021 compared to 2004–2017 provides some evidence that the NH aging is impacted by decadal variability and the limited length of the observation period.

1 Introduction

Anthropogenic greenhouse gas emissions are altering the temperature, dynamics, and composition of the atmosphere at unprecedented rates. Observations from the past several decades show a warming troposphere and a cooling stratosphere (e.g., Steiner et al., 2020), and the consequences of these changes: tropical expansion (e.g., Seidel et al., 2008), an increased tropopause height (e.g., Vallis et al., 2015), and an altered Brewer-Dobson Circulation (BDC) (e.g., Stiller et al., 2017; Bönisch et al., 2011; Fu et al., 2019), amongst others. At the same time, Antarctic ozone recovery in the 21st century following a successful implementation of the Montreal Protocol is warming the Southern hemisphere (SH), and further changing the BDC in a way that is not symmetric between the hemispheres (e.g., Abalos et al., 2019). An understanding of these structural changes to the stratosphere is needed in order to make sense of recent stratospheric trace gas trends. HCl (Mahieu et al., 2014; Strahan et al., 2020), NO_x (Galytska et al., 2019; Dubé et al., 2020), F_y (Prignon et al., 2021), and O_3 (Ball et al., 2018; Bognar et al., 2022) observations all have opposing trends in the SH relative to the Northern hemisphere (NH) in the years since ∼2000.

https://doi.org/10.5194/egusphere-2024-1736
Preprint. Discussion started: 18 July 2024

These trends cannot be explained solely by changes in source gas emissions and there is evidence that they are due to changes in transport by the BDC (e.g., Mahieu et al., 2014; Dubé et al., 2023; Ploeger and Garny, 2022; Prignon et al., 2021; Han et al., 2019).

The BDC is the mechanism for mass transport within the stratosphere. It consists of upwelling in the tropics, poleward transport, and downwelling at mid and high latitudes, as well as quasi-horizontal two-way mixing (Butchart, 2014). Transport within the BDC is commonly quantified by the age of air, which defines the length of time that an air parcel requires to travel from either the surface or the tropopause to some location in the stratosphere (Hall and Plumb, 1994; Waugh and Hall, 2002). The age of air is a distribution (or spectrum) of all possible transit times to a given location. The first moment of the age of air spectrum, the mean stratospheric age of air (AoA), is a metric used to represent the mean transit time of an air parcel to a given point in the stratosphere.

Climate models predict that rising atmospheric greenhouse gas concentrations will lead to an accelerated BDC, and therefore younger air throughout the stratosphere (Li et al., 2018; Abalos et al., 2021). Before ∼2000 this effect was compounded by ozone depletion, which lead to an even greater decrease in AoA in the SH relative to the NH below 10 hPa (Abalos et al., 2019; Polvani et al., 2018). The recovery of the ozone layer in more recent years is expected to produce an opposite effect, resulting in air that is older in the SH relative to NH, which will counteract some of the BDC acceleration from greenhouse gases (Polvani et al., 2018).

Reanalyses are weather forecast models that assimilate historical temperature, pressure, and wind observations to provide a more realistic representation of the atmosphere. AoA can be calculated by using reanalysis fields as input to a Chemical Transport Model (CTM) (e.g., Chipperfield, 2006). Monge-Sanz et al. (2012) were the first to find an increase in AoA in the NH relative to the SH, using the TOMCAT/SLIMCAT CTM (Chipperfield, 2006) driven with ERA-Interim (Dee et al., 2011). Several studies have since shown that AoA trends derived from reanalyses are very different depending upon which reanalysis is considered, regardless of the CTM that is used (Chabrillat et al., 2018; Ploeger and Garny, 2022; Monge-Sanz et al., 2022). However, Ploeger and Garny (2022) found that the hemispheric difference in the AoA trend (the trend in the NH-SH difference) is much more similar amongst the reanalyses than the individual trends in each hemisphere: All four reanalyses that were considered show an aging of the NH relative to the SH over 2005–2017, which is not consistent with the expected response to ozone recovery.

It is not possible to directly measure the AoA, however it can be approximated from observations of a long-lived trace gas with a linearly varying tropospheric source. The most common choices are sulphur hexafluoride (SF_6) and carbon dioxide (CO_2), which are inert in much of the stratosphere, and have well defined tropospheric trends (Waugh and Hall, 2002; Stiller et al., 2008). AoA derived from Michelson Interferometer for Passive Atmospheric Sounding (MIPAS, Fischer et al., 2008) SF_6 observations has a linear change over 2002–2012 that is negative (air getting younger) in the SH and positive (air getting older) in the NH, between 20 and 30 km (Haenel et al., 2015). For the longer time period of 1975–2016, Engel et al. (2017) did not observe a significant AoA trend in the NH based on balloon measurements of CO_2 and SF_6 between 30 hPa and 5 hPa. These results from Engel et al. (2017) are largely inconsistent with the modelled AoA trends presented in Abalos et al. (2021), although the uncertainties in the observations overlap the uncertainties in a few of the model runs.

https://doi.org/10.5194/egusphere-2024-1736
Preprint. Discussion started: 18 July 2024

Attempts to derive AoA from observations of other gases have also been made. Linz et al. (2017) derived AoA from Global OZone Chemistry And Related trace gas Data records for the Stratosphere (GOZCARDS) N_2O observations at 20 km. Their method relied on the relationship between AoA and N_2O, where AoA is derived from aircraft and balloon observations of CO_2. The AoA from N_2O was found to be younger than the AoA from MIPAS SF_6. Linz et al. (2017) did not compare trends in the two AoA versions. Strahan et al. (2020) considered other gases, using HCl and HNO_3 observations from the Network for the Detection of Atmospheric Composition Change (NDACC) to derive the AoA trend. They found that air in the SH became 1 month/decade younger relative to air in the NH over 1994–2018. The longer time period prevents direct comparison, but the pattern of an aging NH relative to the SH is consistent with MIPAS and with results from CTMs driven with various reanalyses (Monge-Sanz et al., 2012; Diallo et al., 2012; Haenel et al., 2015; Ploeger and Garny, 2022).

The limited time period of the MIPAS observations, the limited altitude range of the Linz et al. (2017) N_2O-based AoA, and the sparseness of the balloon measurements used by Engel et al. (2017) motivate the creation of a new observational based AoA dataset that can be used to validate model results. Strahan et al. (2020) provided some new information by deriving AoA trends from HCl and HNO_3, however they used column measurements and so could not compute the AoA as a function of altitude. Their analysis was also limited to the latitudinal resolution of the NDACC stations, and therefore focused on the interhemispheric difference. Our goal in this study is to build on the results of Strahan et al. (2020) by applying their method for calculating the AoA trend to observations from the Atmospheric Chemistry Experiment - Fourier Transform Spectrometer (ACE-FTS, Bernath et al., 2005). By using ACE-FTS observations it is possible to calculate the AoA anomaly and the AoA trend as a function of altitude and latitude. The downside compared to using NDACC observations is that we cannot consider AoA before ACE-FTS began operations in 2004.

The AoA is calculated using ACE-FTS observations of N_2O, CH_4, and $CFC-12$, along with the relationship between the gases and AoA in the Chemical Lagrangian Model of the Stratosphere (CLaMS, McKenna et al., 2002). These gases were chosen as they are long-lived tracers that provide a good representation of dynamic variability in the lower and middle stratosphere. We consider four different sets of CLaMS results, based on inputs from four different reanalyses. The ACE-FTS observations and CLaMS are described in Section 2. Section 3 contains the method for deriving AoA and its trend, along with the corresponding results. A conclusion is given in Section 4.

2 Observations and Model

ACE-FTS is an infrared Fourier transform spectrometer that measures from 750–4400 cm^{-1} (Bernath et al., 2005; Boone et al., 2005). It has been observing the atmosphere from a high inclination orbit on the SCISAT satellite since February 2004. ACE-FTS uses a solar occultation viewing geometry to make approximately 30 atmospheric transmission profile measurements each day, $\sim$15 at sunrise and $\sim$15 at sunset. Vertical profiles of over 40 trace gas species are retrieved from ACE-FTS measurements. We use observations of N_2O, CH_4, and $CFC-12$ from version 4.2 of the retrieval, described in Boone et al. (2020). The observations are filtered according to the data quality flags developed by Sheese et al. (2015) before doing any analysis.

https://doi.org/10.5194/egusphere-2024-1736
Preprint. Discussion started: 18 July 2024

Simulations of N_2O, CH_4, $CFC-12$, and AoA from CLaMS, a Lagrangian chemistry transport model, are also considered. The CLaMS transport scheme includes 3D air parcel trajectory calculations and parameterizations for small-scale atmospheric mixing. AoA is modelled in CLaMS by tracking the time it takes for an inert tracer with a linearly increasing source that is released at the surface to reach a certain location in the stratosphere (Ploeger and Birner, 2016; Ploeger et al., 2021). CLaMS uses a simplified chemistry scheme to model long-lived trace gases (Pommrich et al., 2014).

Reanalysis horizontal winds and diabatic heating rates are provided as input to CLaMS. Four different reanalyses are considered to test the sensitivity of the modelled AoA and gas trends to the input values: The European Centre for Medium-Range Weather Forecasts (ECMWF) interim reanalysis, ERA-Interim (Dee et al., 2011), the ECMWF fifth generation reanalysis, ERA5 (Hersbach et al., 2020), the Modern-Era Retrospective analysis for Research and Applications Version 2, MERRA-2 (Gelaro et al., 2017), and the Japanese 55-year Reanalysis, JRA-55 (Kobayashi et al., 2015).

A detailed discussion of the AoA trends for each reanalysis can be found in Ploeger and Garny (2022). The same CLaMS simulations are used here. The end years of the simulations based on each reanalysis are different, depending on the availability of the reanalysis results. Section 3 focuses on results for 2004–2017 as this is the time period for which both ACE-FTS observations and results from all four reanalyses were available when the model simulations were performed. Results for 2004–2021 are also discussed in the case of ERA5, for which longer simulations are available.

We calculate trends in both the AoA interhemispheric difference (SH−NH) and the latitudinally resolved AoA from N_2O, CH_4, and $CFC-12$. As the focus is on trends due solely to circulation changes, trends caused by changes in surface emissions of the gases need to be accounted for. For the interhemispheric difference we assume that the effect of surface emissions on the trend is the same in both hemispheres and so cancels out, following Strahan et al. (2020). The latitudinally resolved results are based solely on N_2O, and not also CH_4 and $CFC-12$, as N_2O has a well defined tropospheric source trend that has been constant for several decades (Laube et al., 2022; Canadell et al., 2021). This allows us to remove the effect of N_2O emissions on the stratospheric N_2O to get the trend that is only due to changes in stratospheric transport. To do so, a time series of N_2O surface concentrations is required: we use global monthly-mean N_2O measurements from the National Oceanic and Atmospheric Administration Global Monitoring Laboratory (NOAA/GML) Halocarbons and other Atmospheric Trace Species (HATS) flask sampling programme (NOAA/GML, 2022). This dataset combines N_2O observations from 13 stations across the globe.

3 Method and Results

We start by comparing the ACE-FTS measurements and the CLaMS results. This requires interpolating the ACE-FTS profiles from altitude to pressure levels using the pressure profile that is retrieved with each ACE-FTS occultation, and interpolating the CLaMS output to the representative ACE-FTS profile locations and times at 30 km. The individual ACE-FTS and CLaMS profiles are then used to determine the deseasonalized monthly zonal mean (MZM) anomalies at each pressure level. This is calculated by first taking the mean of all data points for a month within a 10 degree latitude band, and then subtracting the multi-annual mean for a given month of the year from all values for that month (i.e. the mean January value is subtracted from

https://doi.org/10.5194/egusphere-2024-1736
Preprint. Discussion started: 18 July 2024

all January values). We focus on mid-latitudes to avoid the effect of polar chemistry, so in all subsequent discussion the SH is defined as 50°S–20°S and the NH is defined as 20°N–50°N. Figure 1 shows the 26.1 hPa MZM anomaly time series of N_2O and AoA for ACE-FTS observations (N_2O only) and for the four CLaMS simulations. A similar plot showing CH_4 and CFC−12 is included in the Appendix, Figure A1. The gaps in the time series are due to the ACE-FTS sampling pattern.

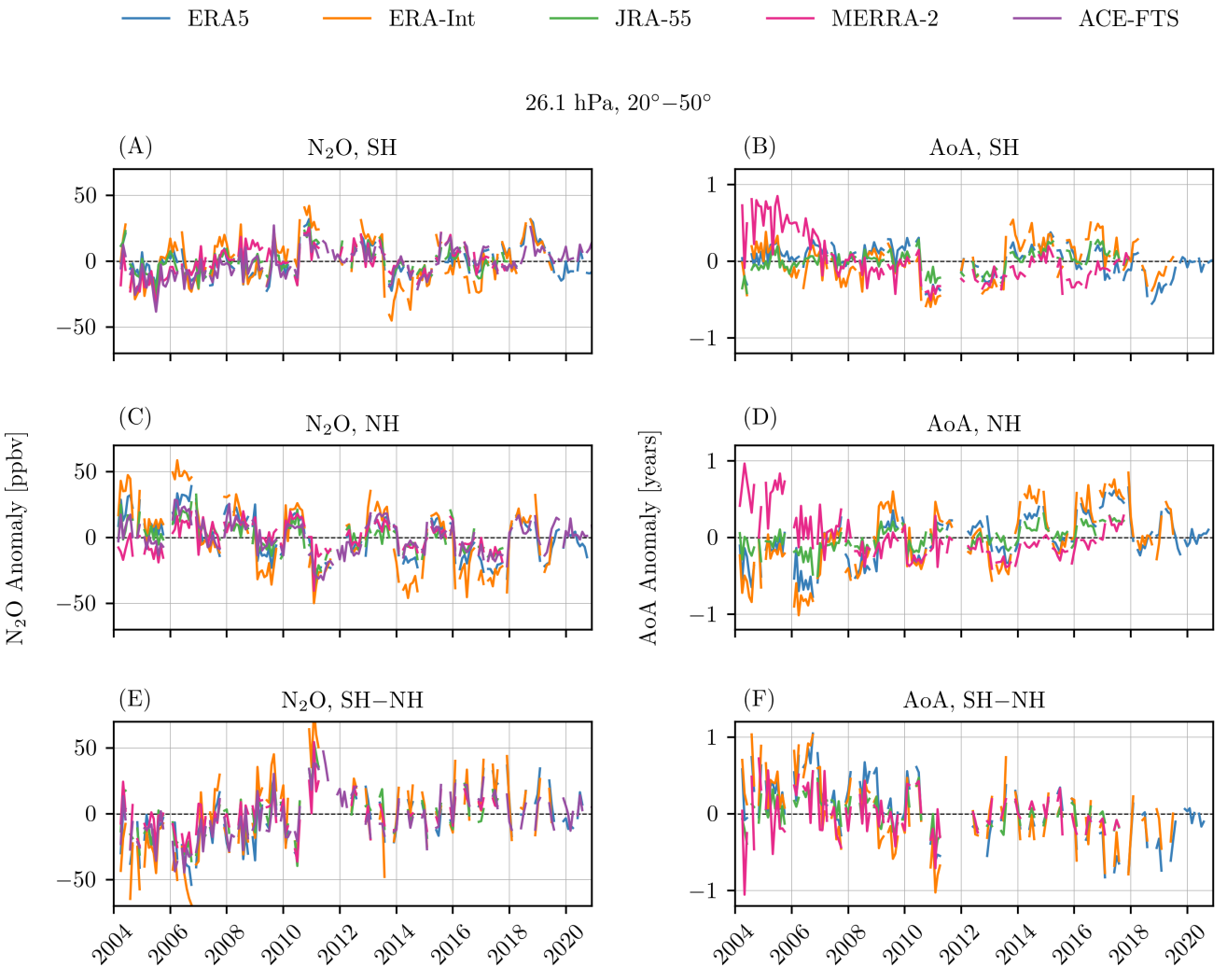

Figure 1. Left: Deseasonalized anomaly time series at 26.1 hPa for ACE-FTS N_2O and N_2O from CLaMS driven with four different reanalyses. Right: Deseasonalized anomaly time series for age of air from CLaMS driven with four different reanalyses. Panels are divided into SH, NH, and SH−NH difference.

https://doi.org/10.5194/egusphere-2024-1736
Preprint. Discussion started: 18 July 2024

Both Figure 1 and appendix Figure A1 show that the MZM ACE-FTS gases and the CLaMS gases from all simulations have very similar variability on a monthly time scale. The correlation of the NH ACE-FTS N_2O and the NH CLaMS N_2O is greater than 0.5 at all levels between 100 hPa and 1 hPa, no matter which CLaMS run is considered. Similar correlation levels also hold in the SH.

Despite the similar short-term variability amongst ACE-FTS and the four model runs, there is a clear difference between the datasets when considering changes over the full 17-year period. For example, in 2004 the NH N_2O anomaly in CLaMS driven with ERA-Interim at 26.1 hPa is nearly 50 ppbv, while the anomaly in MERRA-2 for the same year and level is closer to -10 ppbv. This large difference at the beginning of the time period can result in significantly different trends for each reanalysis. However, there is much less of a bias between ACE-FTS and the different reanalyses when considering the difference between the SH anomaly and the NH anomaly (panels E and F of Figure 1). This was previously shown by Ploeger and Garny (2022), who found that even though AoA trends are very different amongst the reanalyses, the trends in the interhemispheric difference all have a similar structure, with greater aging in the NH relative to the SH during 2005–2017. This suggests that even though the reanalyses do not have the same absolute AoA changes, they are all capturing the AoA changes in a way that is consistent between the hemispheres.

3.1 Trend in AoA Interhemispheric Difference

We start by deriving the trend in the AoA interhemispheric (SH−NH) difference as a function of pressure level, as an update to the results of Strahan et al. (2020), who only considered trends at 52 hPa. This requires assuming that the trace gas observations being used represent dynamical variability in the atmosphere. The level of correlation between AoA and a gas shows the similarity of the month to month variability. The correlation between AoA and N_2O, CH_4, and $CFC-12$ from CLaMS forced with each reanalysis is shown in the top row of Figure 2, while the bottom row of Figure 2 shows the same correlations but using ACE-FTS gases. Note that the ACE-FTS $CFC-12$ observations are only available up to $\sim$8 hPa.

All three gases are strongly anti-correlated with AoA below $\sim$3 hPa. At these levels the gases have long chemical lifetimes so their distributions in the stratosphere are controlled by transport processes, for which AoA is a metric. The anti-correlation occurs because all three gases have tropospheric sources and stratospheric sinks so older air implies the gas has had more time to be removed by chemical processes. Subsequent analysis is limited to levels where all anti-correlations are less than 0.5, implying that there is a strong relationship between AoA and the gas. This corresponds to levels below 3 hPa for N_2O and CH_4, and below 10 hPa for $CFC-12$.

Although the AoA and trace gases simulated by CLaMS are quite different depending on the input reanalysis winds and heating rates, the relationship between AoA and the gases should always be consistent as it largely depends on the chemistry in CLaMS. The top row of Figure 3 illustrates this relationship by showing the slope in the SH−NH difference for AoA with each of N_2O (panel A), CH_4 (panel B), and $CFC-12$ (panel C). The slope is determined by calculating the least-squares fit between the AoA anomaly and the trace gas relative anomaly. The relative anomaly is the anomaly divided by the overall mean and multiplied by 100, so that it is in units of percent. Although the slope for each reanalysis is not within the 2σ error of the least squares fit for every other reanalysis at every altitude, the slopes have a very similar vertical structure and similar values,

https://doi.org/10.5194/egusphere-2024-1736
Preprint. Discussion started: 18 July 2024

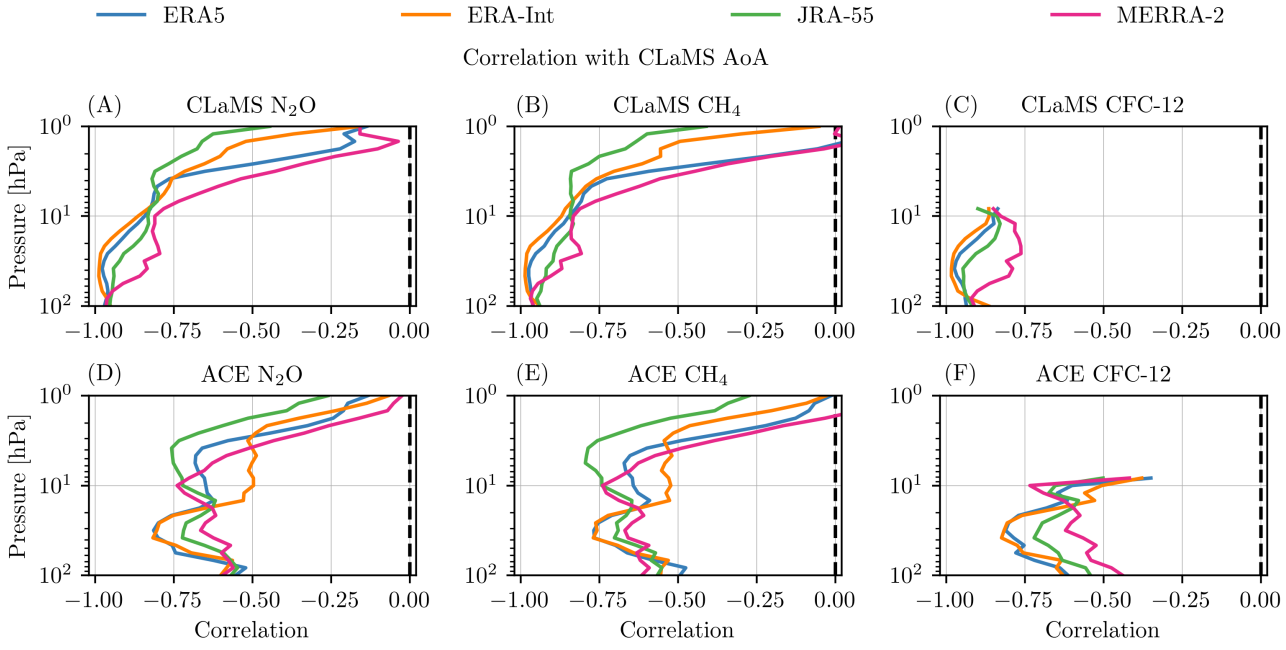

Figure 2. Correlation with AoA from CLaMS driven with four different reanalyses. Top row: Gases from CLaMS. Bottom row: Gases from ACE-FTS. All results for SH−NH difference over 2004–2017. CFC-12 observations from ACE-FTS are only available up to 8 hPa.

no matter which reanalysis is used. The slopes are not the same for each trace gas because the gases are affected by different chemical mechanisms.

To derive the ACE-FTS AoA trend the slope is multiplied by the ACE-FTS trace gas trend,

$$\text{ACE AoA Trend [years/decade]} = \frac{\text{CLaMS AoA [years]}}{\text{CLaMS Gas [\%]}} \times \text{ACE Gas Trend}[\%/\text{decade}]. \quad (1)$$

In this case the ACE-FTS gas trend in the interhemispheric difference is calculated with a simple linear fit to the anomalies. Panels D, E, and F of Figure 3 show these trends for each of N_2O, CH_4, and CFC−12, respectively. The trends are significant where the error bar does not cross the zero line, so between approximately 20 hPa and 80 hPa. At these levels there is a positive trend, so the gases increased more in the SH relative to the NH over 2004–2017.

The resulting trends in the AoA interhemispheric difference, calculated with Equation 1, are shown in the bottom row of Figure 3. The AoA trends have an opposite structure to the trace gas trends, and show that below 10 hPa the SH became significantly younger than the NH during 2004–2017. Table 1 summarizes the AoA trends from each gas at several levels in the middle stratosphere, with results from all four reanalyses averaged together. A key result is that the trends in the AoA interhemispheric differences agree within the regression error regardless of which trace gas is used, and regardless of which reanalysis is used as CLaMS input. Therefore the choice of reanalysis is not important for determining SH−NH AoA trends

https://doi.org/10.5194/egusphere-2024-1736
Preprint. Discussion started: 18 July 2024

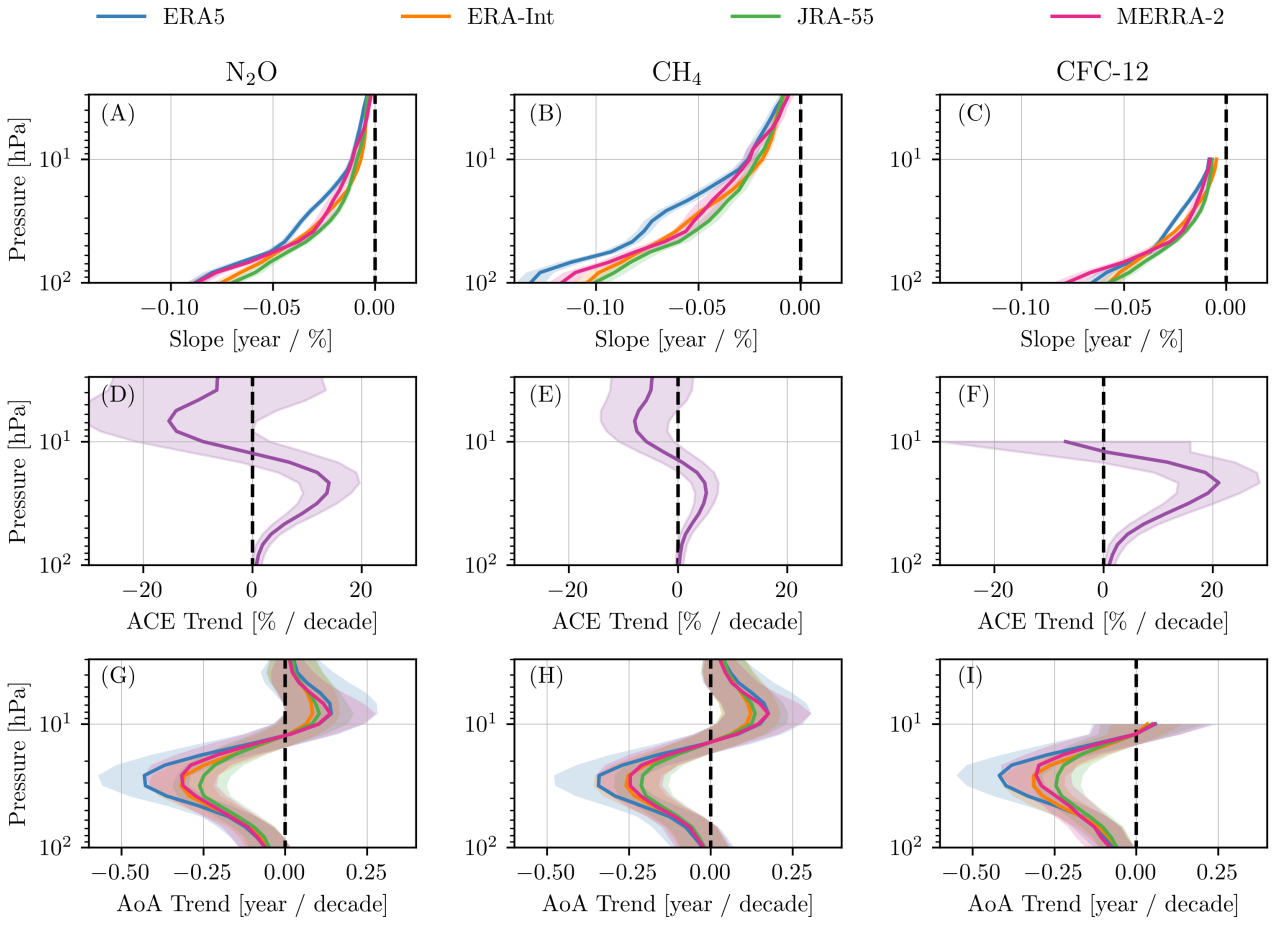

Figure 3. Top: Slope from least-squares fit to CLaMS AoA and corresponding gas. Centre: Trend in ACE-FTS gas. Bottom: Derived AoA trend. All results for SH−NH difference over 2004–2017. Results are shown for CLaMS driven with four different reanalyses. Shaded regions denote the 2σ error.

with this method, and neither are any specifics of the ACE-FTS observations/retrievals that may have different impacts on the three gases considered.

3.2 Global AoA Time Series and Trend Analysis

We now extend the analysis by creating a latitudinally and vertically resolved AoA anomaly time series and using this to better understand the variability in AoA in each hemisphere individually over the past two decades. One complication when deriving AoA as a function of latitude from trace gas observations is that the effect of surface emissions on the gas trend is not

https://doi.org/10.5194/egusphere-2024-1736
Preprint. Discussion started: 18 July 2024

Table 1. Mean trends in AoA interhemispheric difference (SH−NH) for 2004–2017, based on CLaMS input from four different reanalyses. Trend units are year/decade. Errors are the 2σ uncertainty.

Level [hPa]	AoA from N_2O [yr./dec.]	AoA from CH_4 [yr./dec.]	AoA from CFC−12 [yr./dec.]
21.5	-0.28±0.12	-0.21±0.12	-0.29±0.11
31.6	-0.33±0.11	-0.27±0.10	-0.31±0.10
46.4	-0.23±0.09	-0.17±0.09	-0.22±0.08
56.2	-0.16±0.08	-0.11±0.09	-0.16±0.07

automatically removed (see Section 2). To account for this it is necessary to remove the surface emission trend from the trace gas observations before calculating the AoA. This is only possible for N_2O, as N_2O has a relatively constant emission trend since measurements began in 1977 (Canadell et al., 2021). This means that the emission driven contribution to the stratospheric N_2O trends is constant throughout the stratosphere and not modified by variations in transit time. Thus we can simply subtract the emissions trend from ACE-FTS N_2O observations at all altitudes/latitudes. This cannot be done so easily for CH_4 and CFC−12 as their emission rates change significantly depending on the time period considered (Laube et al., 2022; Canadell et al., 2021).

The effect of surface emissions is removed from the ACE-FTS N_2O by subtracting the linear trend in the surface data from the relative anomaly of the ACE-FTS observations in each bin (the same method described in Dubé et al. (2023)). These anomalies are then multiplied by the least squares fit of CLaMS AoA to N_2O (the slope) to get the ACE-FTS AoA anomaly,

$$\text{ACE AoA [years]} = \frac{\text{CLaMS AoA [years]}}{\text{CLaMS Gas [\%]}} \times \text{ACE Gas [\%]}. \tag{2}$$

Here the slope term is different for each altitude and latitude bin. Figure 4 shows that the slopes have the same latitudinal and vertical structure no matter which reanalysis is used in the CLaMS runs. The slope is most negative at lower levels and in the tropics.

The resulting AoA anomaly time series for four sample latitude/altitude bins are shown in Figure 5. Note that results from CLaMS run with ERA5 are available to the end of 2021. The AoA anomalies are very similar for all four reanalyses. One source of variability that stands out, particularly in panel A, is the quasi-biennial oscillation (QBO, Wallace et al., 1993), an oscillation in the tropical zonal winds that has an approximately 2-year period. The QBO phase has previously been shown to affect the age of air spectrum by Ploeger and Birner (2016). To account for variability from the QBO, as well as possible variability from the El-Niño Southern Oscillation and the 11-year solar cycle, we calculate trends in the latitudinally resolved AoA using a multiple linear regression model (MLR).

The MLR model is defined as

$$AoA(t) = \beta + \beta_{trend} \times linear(t) + \beta^{(2)}_{qboa} \times QBO_a(t) + \beta^{(2)}_{qbob} \times QBO_b(t) + \beta_{enso} \times ENSO(t) + \beta_{solar} \times F10.7(t) + R(t). \tag{3}$$

https://doi.org/10.5194/egusphere-2024-1736
Preprint. Discussion started: 18 July 2024

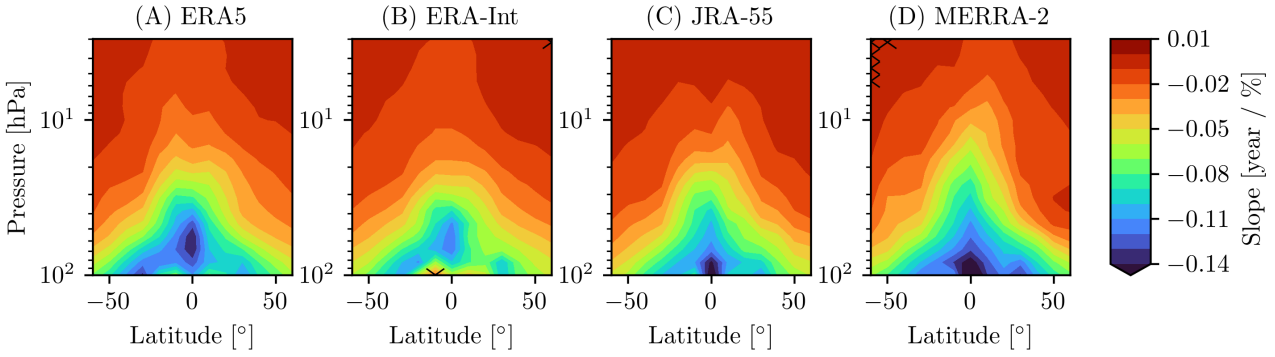

Figure 4. Slope from linear fit to CLaMS AoA and N_2O for 2004–2017. Results are shown for CLaMS driven with four different reanalyses. Hatching denotes statistically insignificant trends at the 2σ level (only MERRA-2 and ERA-Int have hatching, and very few bins are hatched).

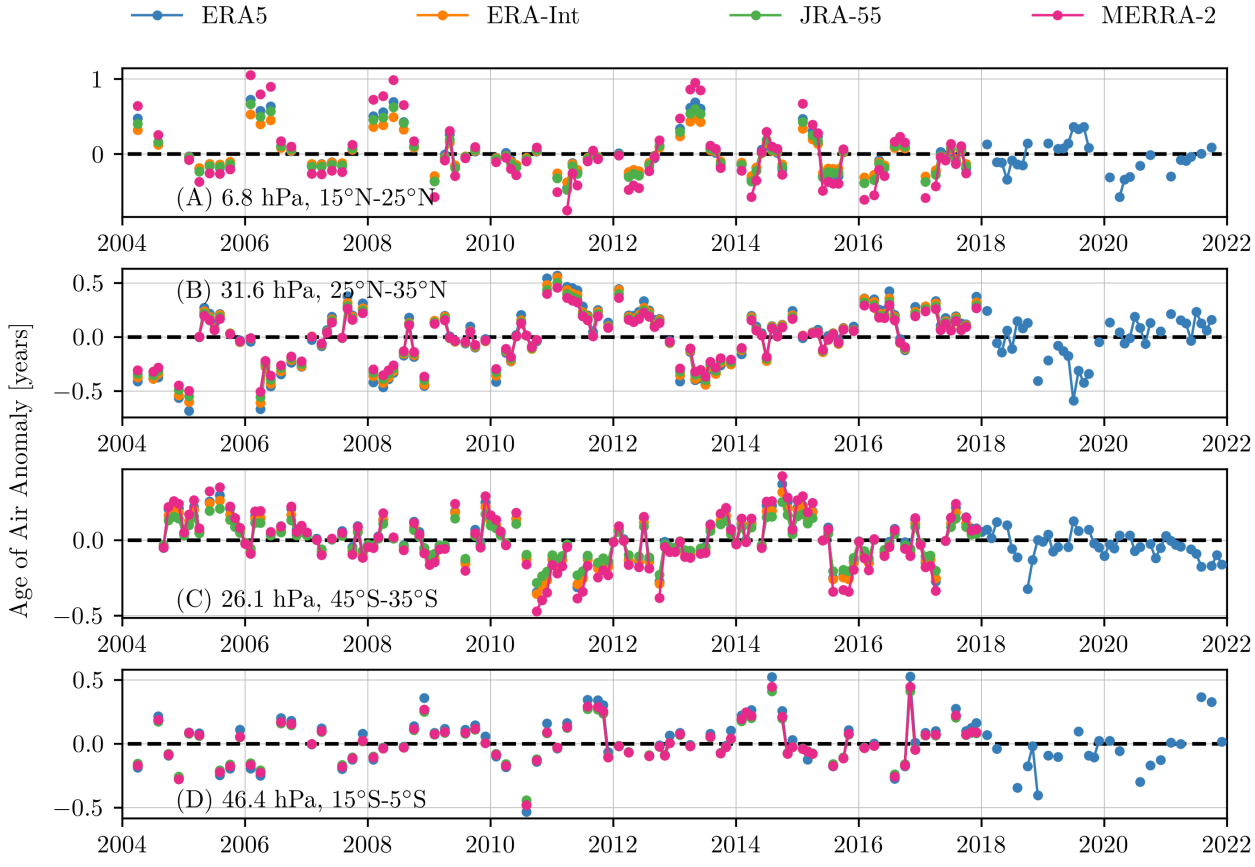

Figure 5. AoA anomaly for four latitude and altitude bins. Results are shown for CLaMS driven with four different reanalyses.

https://doi.org/10.5194/egusphere-2024-1736
Preprint. Discussion started: 18 July 2024

Each β_i defines a regression coefficient, with the superscripts defining the highest seasonal harmonic included for that term. Harmonics are included for the QBO predictors, $QBO_a(t)$ and $QBO_b(t)$, to account for coupling between the QBO and the seasonal cycle. There is no need to include regression terms for annual oscillations as the AoA anomaly is deseasonalized. β_{trend} is the AoA trend in units of years/decade, $F10.7(t)$ is the solar flux at 10.7 cm, $ENSO(t)$ is the El-Niño Southern Oscillation index, $QBO_a(t)$ and $QBO_b(t)$ are the first two principal components of the monthly mean zonal winds measured in Singapore, and $R(t)$ is the residual. Further details on the regression model and the proxy data sources are provided in Damadeo et al. (2022).

The AoA trends over 2004–2017 are compared for each reanalysis in Figure 6. As expected, there is a significant hemispheric asymmetry in the trends. Below 10 hPa, most of this asymmetry is coming from aging of up to 0.4 years/decade in the NH. The positive AoA trend in the NH is consistent with reanalysis results from Monge-Sanz et al. (2022). The AoA trend in the SH is largely insignificant, except for between 10 hPa and 30 hPa at latitudes $>-40°$, where the air is getting younger by up to 0.2 years/decade. Above 10 hPa the NH is getting younger relative to the SH. As expected, given the consistency of the AoA time series derived from each reanalysis, the AoA trends are very similar in all four cases, although ERA5 has slightly more NH aging below 10 hPa. The region of highest positive trend in the NH corresponds to panel B in Figure 5, and the region of most negative trend in the SH corresponds to panel C.

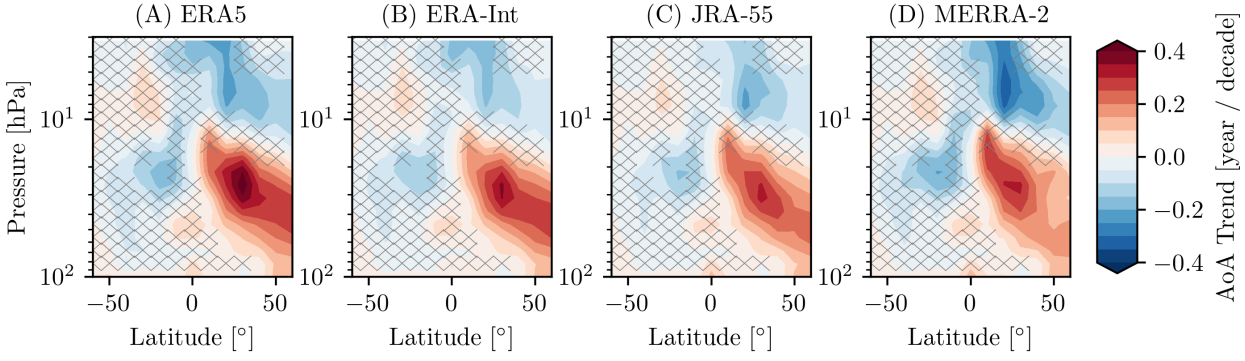

Figure 6. AoA trends for 2004–2017. Results are shown for CLaMS driven with four different reanalyses. Hatching denotes statistically insignificant trends at the 2σ level.

The QBO, solar, and ENSO coefficients, along with the goodness of fit (R^2) values, are provided in the Appendix Figure A2. The QBO is a significant source of variability for AoA, particularly in the tropics. The solar cycle and ENSO have minimal impacts on stratospheric AoA. There are clearly some unaccounted for sources of variability as at most 60% of the variability in AoA is explained by the regression model in the tropics, and 30% at higher latitudes. This is a source of uncertainty in the AoA trends as there could be some unknown source of decadal variability influencing the trends.

Figure 6 shows the AoA trends from 2004–2017 so that trends derived from CLaMS forced with four different reanalyses could be compared. However, results from CLaMS forced with ERA5 inputs are available to the end of 2021. AoA trends derived from these results, Figure 7, show a weakened hemispheric asymmetry: including four more years in the analysis

https://doi.org/10.5194/egusphere-2024-1736
Preprint. Discussion started: 18 July 2024

results in a smaller rate of NH aging between 10 and 70 hPa. This shows that AoA trends in the middle stratosphere depend strongly on the period that is considered. Caution should therefore be taken when comparing the AoA trend to results from earlier studies that do not use the exact same time period for the trend calculation.

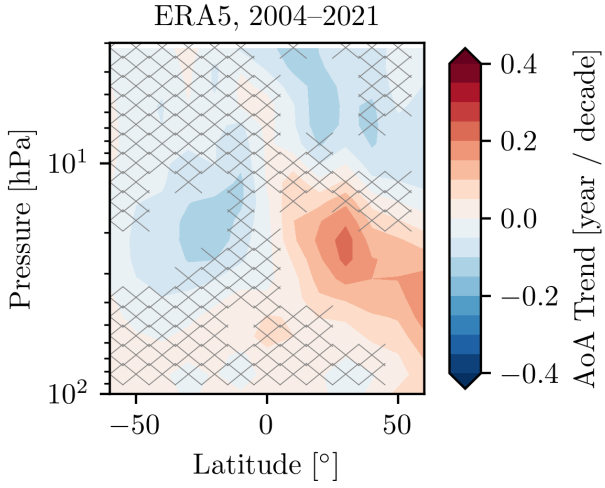

Figure 7. AoA trends for 2004–2021. Results are shown for CLaMS driven with ERA5. Hatching denotes statistically insignificant trends at the 2σ level.

4 Conclusions

Recent observations (since ∼2000) of stratospheric trace gases have opposing signs in the NH compared to the SH, which Ploeger and Garny (2022) attributed to structural changes in the BDC. One metric for quantifying the transport rate of air by the BDC, including transport from upwelling and mixing, is the AoA. Quantifying AoA trends is useful for understanding how much of the trace gas trends are caused by circulation changes, as opposed to changes in the source gases or chemical reaction rates. The AoA can be readily modelled, but it is more difficult to determine from observations. All existing observation-based AoA records have some limitation: AoA from MIPAS SF_6 is only available for 10 years, AoA from balloon observations is sparse in latitude and time (Engel et al., 2017), AoA from GOZCARDS N_2O is limited in altitude (Linz et al., 2017), and AoA from NDACC HCl and HNO_3 is limited in both altitude and latitude (Strahan et al., 2020). Thus the goal of the present study is to provide a new estimate of AoA and AoA trends using ACE-FTS observations, which have very good vertical resolution (1–2 km) and better latitudinal resolution (monthly global sampling) than ground-based and in-situ measurements, in addition to a nearly 20-year record.

We derived AoA trends using observations of N_2O, CH_4, and CFC−12 from ACE-FTS, along with simulations of the gases and AoA from CLaMS forced with four different reanalyses. We found that, irrespective of which trace gas or reanalysis was used, air in the NH middle stratosphere aged by up to ∼0.3±0.1 years/decade relative to the SH over 2004–2017 near 30 hPa.

https://doi.org/10.5194/egusphere-2024-1736
Preprint. Discussion started: 18 July 2024

The AoA interhemispheric difference trend was smaller at higher and lower levels, but remained significant between 20 hPa and 80 hPa. This trend is primarily driven by aging in the NH, rather than a decrease in age in the SH. We also found that including four more years in the trend calculation, up to 2021, resulted in a smaller NH aging rate in the middle stratosphere and more equal contributions from each hemisphere to the interhemispheric difference trend.

Our finding of aging in the NH relative to the SH is consistent with earlier observational results from e.g., Strahan et al. (2020); Prignon et al. (2021); Haenel et al. (2015), but the different analysis periods used in each study makes it difficult to directly compare the AoA trends. Strahan et al. (2020) found that the NH aged relative to the SH by 1 month/decade (0.08 years/decade) over 1994–2018 and at 52 hPa, with the majority of the trend coming from air getting younger in the SH. This is a smaller AoA interhemispheric difference trend than we find near 52 hPa for the shorter period of 2004–2017, and is also caused by changes in the opposite hemisphere. By beginning their analysis in 1994, rather than after 2000, the results of Strahan et al. (2020) were likely affected by ozone depletion. Polvani et al. (2018) showed that prior to 2000 there was a greater AoA decrease in the SH compared to the NH due to ozone loss, and concluded that it is best to look at AoA trends before and after 2000, as is done in ozone trend studies. As our results are focused on the ozone recovery period, we see less of a reduction in the SH AoA than Strahan et al. (2020).

In general, models predict that stratospheric air will get younger throughout the 21st century, but the decrease in AoA will be small in comparison to the decrease in AoA that occurred in the second half of the 20th century (Polvani et al., 2018; Abalos et al., 2021; Ploeger and Garny, 2022). Abalos et al. (2021) showed that AoA trends are highly sensitive to internal variability, and that at least 20 years are needed to calculate robust AoA trends. Similarly, Ploeger and Garny (2022) found a large inter-model spread in AoA trends over less than 40 years. Our results based on ACE-FTS observations are therefore not necessarily inconsistent with model predictions of air getting younger in both hemispheres as they are only based on 13 years (and in one case 17 years) of measurements. The smaller aging trend in the NH middle stratosphere that we find when AoA trends are calculated over 2004–2021 instead of 2004–2017 provides some evidence that the NH middle stratosphere aging is only a feature of the short observation period and likely related to natural variability, and that the agreement between observations and models can improve with a longer data record.

Code and data availability. ACE-FTS data are available by registration at https://databace.scisat.ca/level2/ (ACE-FTS, 2022).

ACE-FTS data quality flags are available from https://doi.org/10.5683/SP2/BC4AT (Sheese and Walker, 2022).

The NOAA/GML HATS N_2O is available at https://gml.noaa.gov/hats/combined/N2O.html (NOAA/GML, 2022).

The LOTUS regression code and documentation is available at https://arg.usask.ca/docs/LOTUS_regression/index.html (Damadeo et al., 2022).

The monthly zonal mean ACE-FTS AoA anomalies derived from N_2O are available at https://doi.org/10.5281/zenodo.11492264 (Dubé et al., 2024).

The CLaMS model results are available upon request from Felix Ploeger (f.ploeger@fz-juelich.de).

https://doi.org/10.5194/egusphere-2024-1736
Preprint. Discussion started: 18 July 2024

Appendix A: Extra Figures

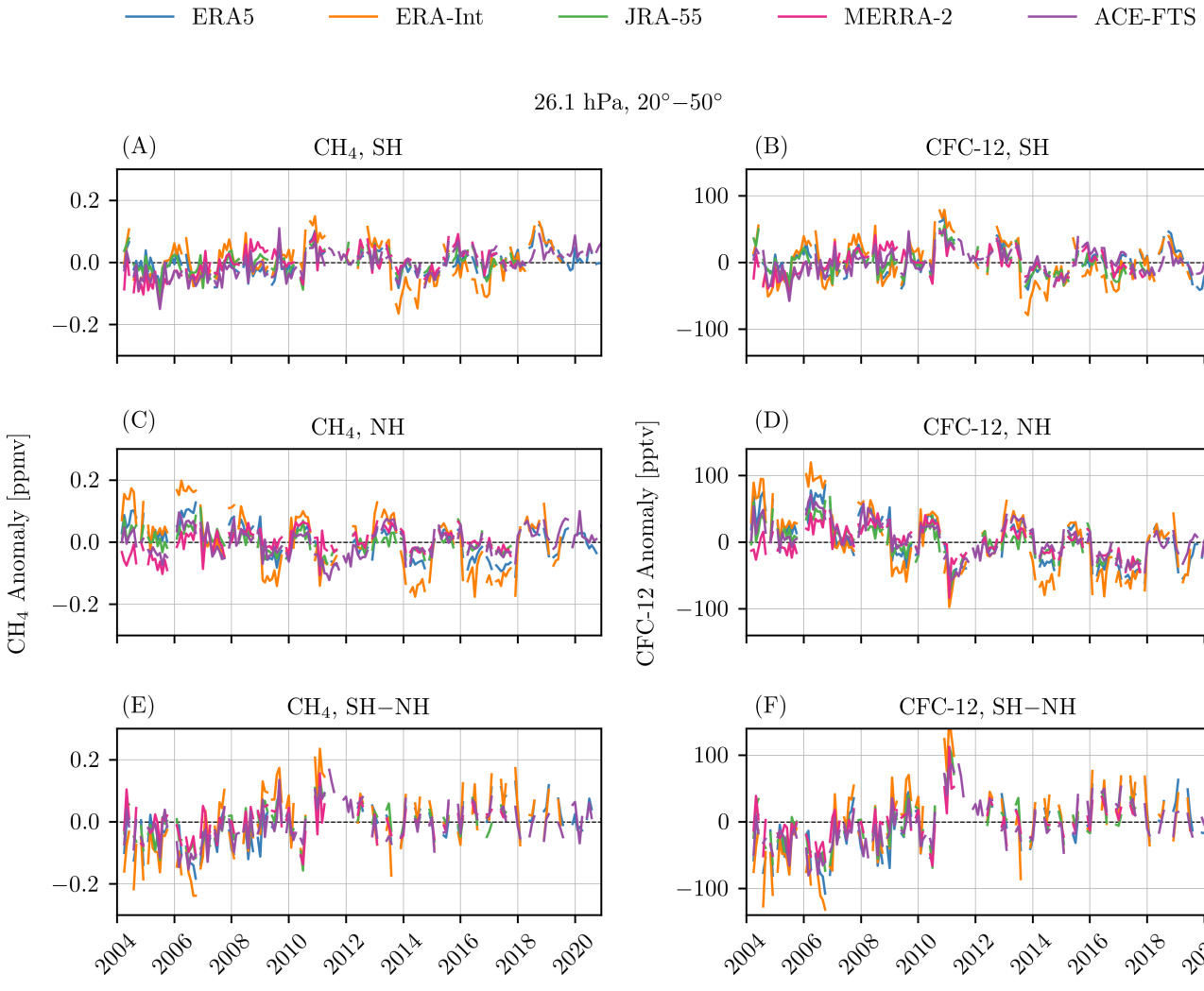

Figure A1. Left: Deseasonalized anomaly time series at 26.1 hPa for ACE-FTS CH_4 and CH_4 from CLaMS driven with four different reanalyses. Right: same as left panels but for CFC−12. Panels are divided into SH, NH, and SH−NH difference.

https://doi.org/10.5194/egusphere-2024-1736
Preprint. Discussion started: 18 July 2024

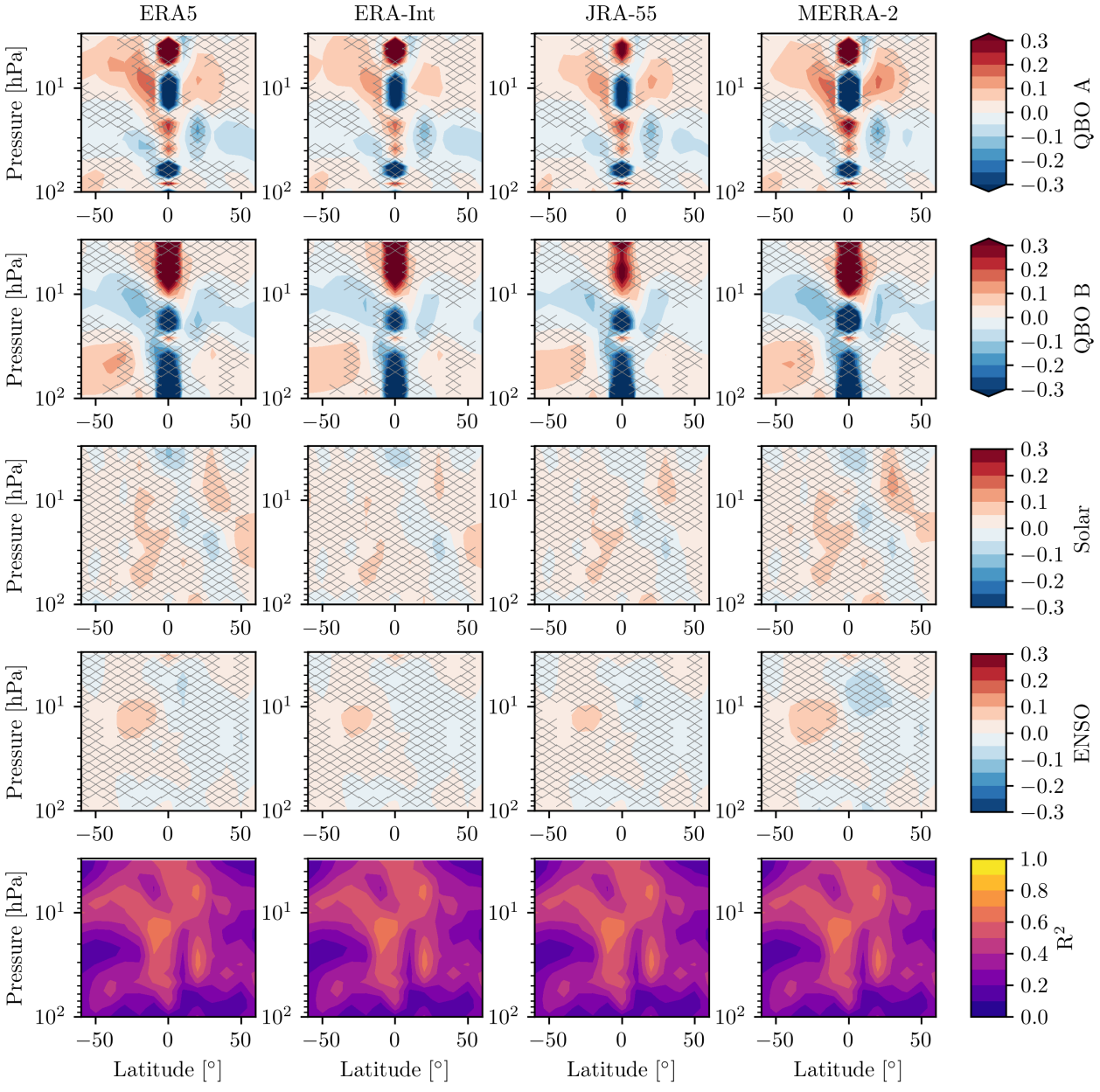

Figure A2. Rows 1–4: Regression coefficients for 2004–2017. Hatching denotes statistically insignificant values at the 2σ level. Row 5: R^2 values for the regression.

https://doi.org/10.5194/egusphere-2024-1736
Preprint. Discussion started: 18 July 2024

Author contributions. KD performed the analysis and wrote the manuscript, with input from all co-authors. ST conceptualized and supervised the project. FP provided the CLaMS simulations. KW provided advice on the ACE-FTS data.

Competing interests. We declare that none of the authors have any competing interests.

Acknowledgements. This research has been supported by the Canadian Space Agency (grant no. 21SUASULSO). The Atmospheric Chemistry Experiment (ACE) is a Canadian-led mission mainly supported by the CSA and the NSERC, and Peter Bernath is the principal investigator.

https://doi.org/10.5194/egusphere-2024-1736
Preprint. Discussion started: 18 July 2024

References

Abalos, M., Polvani, L., Calvo, N., Kinnison, D., Ploeger, F., Randel, W., and Solomon, S.: New Insights on the Impact of Ozone-Depleting Substances on the Brewer-Dobson Circulation, Journal of Geophysical Research: Atmospheres, 124, 2435–2451, https://doi.org/https://doi.org/10.1029/2018JD029301, 2019.

Abalos, M., Calvo, N., Benito-Barca, S., Garny, H., Hardiman, S. C., Lin, P., Andrews, M. B., Butchart, N., Garcia, R., Orbe, C., Saint-Martin, D., Watanabe, S., and Yoshida, K.: The Brewer–Dobson circulation in CMIP6, Atmospheric Chemistry and Physics, 21, 13 571–13 591, https://doi.org/10.5194/acp-21-13571-2021, 2021.

ACE-FTS: Level 2 Data, Version 4.1/4.2, https://databace.scisat.ca/level2/, accessed: 2022-10-05, 2022.

Ball, W. T., Alsing, J., Mortlock, D. J., Staehelin, J., Haigh, J. D., Peter, T., Tummon, F., Stübi, R., Stenke, A., Anderson, J., Bourassa, A., Davis, S. M., Degenstein, D., Frith, S., Froidevaux, L., Roth, C., Sofieva, V., Wang, R., Wild, J., Yu, P., Ziemke, J. R., and Rozanov, E. V.: Evidence for a continuous decline in lower stratospheric ozone offsetting ozone layer recovery, Atmospheric Chemistry and Physics, 18, 1379–1394, https://doi.org/10.5194/acp-18-1379-2018, 2018.

Bernath, P. F., McElroy, C. T., Abrams, M. C., Boone, C. D., Butler, M., Camy-Peyret, C., Carleer, M., Clerbaux, C., Coheur, P.-F., Colin, R., DeCola, P., DeMazière, M., Drummond, J. R., Dufour, D., Evans, W. F. J., Fast, H., Fussen, D., Gilbert, K., Jennings, D. E., Llewellyn, E. J., Lowe, R. P., Mahieu, E., McConnell, J. C., McHugh, M., McLeod, S. D., Michaud, R., Midwinter, C., Nassar, R., Nichitiu, F., Nowlan, C., Rinsland, C. P., Rochon, Y. J., Rowlands, N., Semeniuk, K., Simon, P., Skelton, R., Sloan, J. J., Soucy, M.-A., Strong, K., Tremblay, P., Turnbull, D., Walker, K. A., Walkty, I., Wardle, D. A., Wehrle, V., Zander, R., and Zou, J.: Atmospheric Chemistry Experiment (ACE): Mission overview, Geophysical Research Letters, 32, https://doi.org/https://doi.org/10.1029/2005GL022386, 2005.

Bognar, K., Tegtmeier, S., Bourassa, A., Roth, C., Warnock, T., Zawada, D., and Degenstein, D.: Stratospheric ozone trends for 1984–2021 in the SAGE II–OSIRIS–SAGE III/ISS composite dataset, Atmospheric Chemistry and Physics, 22, 9553–9569, https://doi.org/10.5194/acp-22-9553-2022, 2022.

Bönisch, H., Engel, A., Birner, T., Hoor, P., Tarasick, D. W., and Ray, E. A.: On the structural changes in the Brewer-Dobson circulation after 2000, Atmospheric Chemistry and Physics, 11, 3937–3948, https://doi.org/10.5194/acp-11-3937-2011, 2011.

Boone, C., Bernath, P., Cok, D., Jones, S., and Steffen, J.: Version 4 retrievals for the atmospheric chemistry experiment Fourier transform spectrometer (ACE-FTS) and imagers, Journal of Quantitative Spectroscopy and Radiative Transfer, 247, 106 939, https://doi.org/https://doi.org/10.1016/j.jqsrt.2020.106939, 2020.

Boone, C. D., Nassar, R., Walker, K. A., Rochon, Y., McLeod, S. D., Rinsland, C. P., and Bernath, P. F.: Retrievals for the atmospheric chemistry experiment Fourier-transform spectrometer, Appl. Opt., 44, 7218–7231, https://doi.org/10.1364/AO.44.007218, 2005.

Butchart, N.: The Brewer-Dobson circulation, Reviews of Geophysics, 52, 157–184, https://doi.org/https://doi.org/10.1002/2013RG000448, 2014.

Canadell, J. G., Monteiro, P. M., Costa, M. H., da Cunha, L. C., Cox, P. M., Eliseev, A. V., Henson, S., Ishii, M., Jaccard, S., Koven, C., Lohila, A., Patra, P. K., Piao, S., Rogelj, J., Syampungani, S., Zaehle, S., and Zickfeld, K.: Global Carbon and other Biogeochemical Cycles and Feedbacks, in: Climate Change 2021: The Physical Science Basis. Contribution of Working Group I to the Sixth Assessment Report of the Intergovernmental Panel on Climate Change, edited by Masson-Delmotte, V., Zhai, P., Pirani, A., Connors, S. L., Péan, C., Berger, S., N. Caud, Y. C., Goldfarb, L., Gomis, M. I., Huang, M., Leitzell, K., Lonnoy, E., Matthews, J. B. R., Maycock, T. K., Waterfield, T., Yelekçi, O., Yu, R., and Zhou, B., chap. 5, p. 673–816, Cambridge University Press, https://doi.org/doi:10.1017/9781009157896.007, 2021.

https://doi.org/10.5194/egusphere-2024-1736
Preprint. Discussion started: 18 July 2024

Chabrillat, S., Vigouroux, C., Christophe, Y., Engel, A., Errera, Q., Minganti, D., Monge-Sanz, B. M., Segers, A., and Mahieu, E.: Comparison of mean age of air in five reanalyses using the BASCOE transport model, Atmospheric Chemistry and Physics, 18, 14 715–14 735, https://doi.org/10.5194/acp-18-14715-2018, 2018.

Chipperfield, M. P.: New version of the TOMCAT/SLIMCAT off-line chemical transport model: Intercomparison of stratospheric tracer experiments, Quarterly Journal of the Royal Meteorological Society, 132, 1179–1203, https://doi.org/https://doi.org/10.1256/qj.05.51, 2006.

Damadeo, R., Hassler, B., Zawada, D., Frith, S., Ball, W., Chang, K., Degenstein, D., Hubert, D., Misois, S., Petropavlovskikh, I., Roth, C., Sofieva, V., Steinbrecht, W., Tourpali, K., Zerefos, C., Alsing, J., Balis, D., Coldewey-Egbers, M., Eleftheratos, K., Godin-Beekmann, S., Gruzdev, A., Kapsomenakis, J., Laeng, A., Laine, M., Maillard Barras, E., Taylor, M., von Clarmann, T., Weber, M., and Wild, J.: LOTUS Regression Code, SPARC LOTUS Activity, https://github.com/usask-arg/lotus-regression, accessed: 2024-02-23, 2022.

Dee, D. P., Uppala, S. M., Simmons, A. J., Berrisford, P., Poli, P., Kobayashi, S., Andrae, U., Balmaseda, M. A., Balsamo, G., Bauer, P., Bechtold, P., Beljaars, A. C. M., van de Berg, L., Bidlot, J., Bormann, N., Delsol, C., Dragani, R., Fuentes, M., Geer, A. J., Haimberger, L., Healy, S. B., Hersbach, H., Hólm, E. V., Isaksen, L., Kållberg, P., Köhler, M., Matricardi, M., McNally, A. P., Monge-Sanz, B. M., Morcrette, J.-J., Park, B.-K., Peubey, C., de Rosnay, P., Tavolato, C., Thépaut, J.-N., and Vitart, F.: The ERA-Interim reanalysis: configuration and performance of the data assimilation system, Quarterly Journal of the Royal Meteorological Society, 137, 553–597, https://doi.org/https://doi.org/10.1002/qj.828, 2011.

Diallo, M., Legras, B., and Chédin, A.: Age of stratospheric air in the ERA-Interim, Atmospheric Chemistry and Physics, 12, 12 133–12 154, https://doi.org/10.5194/acp-12-12133-2012, 2012.

Dubé, K., Randel, W., Bourassa, A., Zawada, D., McLinden, C., and Degenstein, D.: Trends and Variability in Stratospheric NOx Derived From Merged SAGE II and OSIRIS Satellite Observations, Journal of Geophysical Research: Atmospheres, 125, e2019JD031 798, https://doi.org/https://doi.org/10.1029/2019JD031798, 2020.

Dubé, K., Tegtmeier, S., Bourassa, A., Zawada, D., Degenstein, D., Sheese, P. E., Walker, K. A., and Randel, W.: N_2O as a regression proxy for dynamical variability in stratospheric trace gas trends, Atmospheric Chemistry and Physics, 23, 13 283–13 300, https://doi.org/10.5194/acp-23-13283-2023, 2023.

Dubé, K., Tegtmeier, S., Ploeger, F., and Walker, K. A.: Mean age of air anomaly derived from ACE-FTS N2O, https://doi.org/https://doi.org/10.5281/zenodo.11492264, 2024.

Engel, A., Bönisch, H., Ullrich, M., Sitals, R., Membrive, O., Danis, F., and Crevoisier, C.: Mean age of stratospheric air derived from AirCore observations, Atmospheric Chemistry and Physics, 17, 6825–6838, https://doi.org/10.5194/acp-17-6825-2017, 2017.

Fischer, H., Birk, M., Blom, C., Carli, B., Carlotti, M., von Clarmann, T., Delbouille, L., Dudhia, A., Ehhalt, D., Endemann, M., Flaud, J. M., Gessner, R., Kleinert, A., Koopman, R., Langen, J., López-Puertas, M., Mosner, P., Nett, H., Oelhaf, H., Perron, G., Remedios, J., Ridolfi, M., Stiller, G., and Zander, R.: MIPAS: an instrument for atmospheric and climate research, Atmospheric Chemistry and Physics, 8, 2151–2188, https://doi.org/10.5194/acp-8-2151-2008, 2008.

Fu, Q., Solomon, S., Pahlavan, H. A., and Lin, P.: Observed changes in Brewer–Dobson circulation for 1980–2018, Environmental Research Letters, 14, 114 026, https://doi.org/10.1088/1748-9326/ab4de7, 2019.

Galytska, E., Rozanov, A., Chipperfield, M. P., Dhomse, Weber, M., Arosio, C., Feng, W., and Burrows, J. P.: Dynamically controlled ozone decline in the tropical mid-stratosphere observed by SCIAMACHY, Atmospheric Chemistry and Physics, 19, 767–783, https://doi.org/10.5194/acp-19-767-2019, 2019.

https://doi.org/10.5194/egusphere-2024-1736
Preprint. Discussion started: 18 July 2024

Gelaro, R., McCarty, W., Suárez, M. J., Todling, R., Molod, A., Takacs, L., Randles, C. A., Darmenov, A., Bosilovich, M. G., Reichle, R., Wargan, K., Coy, L., Cullather, R., Draper, C., Akella, S., Buchard, V., Conaty, A., da Silva, A. M., Gu, W., Kim, G.-K., Koster, R., Lucchesi, R., Merkova, D., Nielsen, J. E., Partyka, G., Pawson, S., Putman, W., Rienecker, M., Schubert, S. D., Sienkiewicz, M., and Zhao, B.: The Modern-Era Retrospective Analysis for Research and Applications, Version 2 (MERRA-2), Journal of Climate, 30, 5419 – 5454, https://doi.org/https://doi.org/10.1175/JCLI-D-16-0758.1, 2017.

Haenel, F. J., Stiller, G. P., von Clarmann, T., Funke, B., Eckert, E., Glatthor, N., Grabowski, U., Kellmann, S., Kiefer, M., Linden, A., and Reddmann, T.: Reassessment of MIPAS age of air trends and variability, Atmospheric Chemistry and Physics, 15, 13 161–13 176, https://doi.org/10.5194/acp-15-13161-2015, 2015.

Hall, T. M. and Plumb, R. A.: Age as a diagnostic of stratospheric transport, Journal of Geophysical Research: Atmospheres, 99, 1059–1070, https://doi.org/https://doi.org/10.1029/93JD03192, 1994.

Han, Y., Tian, W., Chipperfield, M. P., Zhang, J., Wang, F., Sang, W., Luo, J., Feng, W., Chrysanthou, A., and Tian, H.: Attribution of the Hemispheric Asymmetries in Trends of Stratospheric Trace Gases Inferred From Microwave Limb Sounder (MLS) Measurements, Journal of Geophysical Research: Atmospheres, 124, 6283–6293, https://doi.org/https://doi.org/10.1029/2018JD029723, 2019.

Hersbach, H., Bell, B., Berrisford, P., Hirahara, S., Horányi, A., Muñoz-Sabater, J., Nicolas, J., Peubey, C., Radu, R., Schepers, D., Simmons, A., Soci, C., Abdalla, S., Abellan, X., Balsamo, G., Bechtold, P., Biavati, G., Bidlot, J., Bonavita, M., De Chiara, G., Dahlgren, P., Dee, D., Diamantakis, M., Dragani, R., Flemming, J., Forbes, R., Fuentes, M., Geer, A., Haimberger, L., Healy, S., Hogan, R. J., Hólm, E., Janisková, M., Keeley, S., Laloyaux, P., Lopez, P., Lupu, C., Radnoti, G., de Rosnay, P., Rozum, I., Vamborg, F., Villaume, S., and Thépaut, J.-N.: The ERA5 global reanalysis, Quarterly Journal of the Royal Meteorological Society, 146, 1999–2049, https://doi.org/https://doi.org/10.1002/qj.3803, 2020.

Kobayashi, S., Ota, Y., Harada, Y., Ebita, A., Moriya, M., Onoda, H., Onogi, K., Kamahori, H., Kobayashi, C., Endo, H., et al.: The JRA-55 reanalysis: General specifications and basic characteristics, Journal of the Meteorological Society of Japan. Ser. II, 93, 5–48, https://doi.org/https://doi.org/10.2151/jmsj.2015-001, 2015.

Laube, J., Tegtmeier, S., Fernandez, R., Harrison, J., Hu, L., Krummel, P., Mahieu, E., Park, S., and Western, L.: Update on Ozone-Depleting Substances (ODSs) and Other Gases of Interest to the Montreal Protocol, in: Scientific Assessment of Ozone Depletion: 2022, GAW Report No. 278, chap. 1, pp. 53–113, WMO, Geneva, Switzerland, 2022.

Li, F., Newman, P., Pawson, S., and Perlwitz, J.: Effects of Greenhouse Gas Increase and Stratospheric Ozone Depletion on Stratospheric Mean Age of Air in 1960–2010, Journal of Geophysical Research: Atmospheres, 123, 2098–2110, https://doi.org/https://doi.org/10.1002/2017JD027562, 2018.

Linz, M., Plumb, R. A., Gerber, E. P., Haenel, F. J., Stiller, G., Kinnison, D. E., Ming, A., and Neu, J. L.: The strength of the meridional overturning circulation of the stratosphere, Nature Geoscience, 10, 663–667, https://doi.org/https://doi.org/10.1038/ngeo3013, 2017.

Mahieu, E., Chipperfield, M., Notholt, J., Reddmann, T., Anderson, J., Bernath, P., Blumenstock, T., Coffey, M., Dhomse, S., Feng, W., et al.: Recent Northern Hemisphere stratospheric HCl increase due to atmospheric circulation changes, Nature, 515, 104–107, https://doi.org/10.1038/nature13857, 2014.

McKenna, D. S., Konopka, P., Grooß, J.-U., Günther, G., Müller, R., Spang, R., Offermann, D., and Orsolini, Y.: A new Chemical Lagrangian Model of the Stratosphere (CLaMS) 1. Formulation of advection and mixing, Journal of Geophysical Research: Atmospheres, 107, ACH 15–1–ACH 15–15, https://doi.org/https://doi.org/10.1029/2000JD000114, 2002.

Monge-Sanz, B., Birner, T., Chabrillat, S., Diallo, M., Haenel, F., Konopka, P., Legras, B., Ploeger, F., Reddmann, T., Stiller, G., Wright, J., Abalos, M., Boenisch, H., Davis, S., Garny, H., Hitchcock, P., Miyazaki, K., Roscoe, H., Sato, K., Tao, M., and Waugh, D.: Brewer-

https://doi.org/10.5194/egusphere-2024-1736
Preprint. Discussion started: 18 July 2024

Dobson Circulation., in: SPARC 2022: SPARC Reanalysis Intercomparison Project (S-RIP) Final Report, edited by Fujiwara, M., Manney, G., Gray, L. J., and Wright, J. S., chap. 5, pp. 165–219, https://doi.org/10.17874/800dee57d13, 2022.

Monge-Sanz, B. M., Chipperfield, M. P., Dee, D. P., Simmons, A. J., and Uppala, S. M.: Improvements in the stratospheric transport achieved by a chemistry transport model with ECMWF (re)analyses: identifying effects and remaining challenges, Quarterly Journal of the Royal Meteorological Society, 139, 654–673, https://doi.org/https://doi.org/10.1002/qj.1996, 2012.

NOAA/GML: Nitrous Oxide (N_2O) - Combined Dataset, https://gml.noaa.gov/hats/combined/N2O.html, accessed: 2022-11-04, 2022.

Ploeger, F. and Birner, T.: Seasonal and inter-annual variability of lower stratospheric age of air spectra, Atmospheric Chemistry and Physics, 16, 10 195–10 213, https://doi.org/10.5194/acp-16-10195-2016, 2016.

Ploeger, F. and Garny, H.: Hemispheric asymmetries in recent changes in the stratospheric circulation, Atmospheric Chemistry and Physics, 22, 5559–5576, https://doi.org/10.5194/acp-22-5559-2022, 2022.

Ploeger, F., Diallo, M., Charlesworth, E., Konopka, P., Legras, B., Laube, J. C., Grooß, J.-U., Günther, G., Engel, A., and Riese, M.: The stratospheric Brewer–Dobson circulation inferred from age of air in the ERA5 reanalysis, Atmospheric Chemistry and Physics, 21, 8393–8412, https://doi.org/10.5194/acp-21-8393-2021, 2021.

Polvani, L. M., Abalos, M., Garcia, R., Kinnison, D., and Randel, W. J.: Significant Weakening of Brewer-Dobson Circulation Trends Over the 21st Century as a Consequence of the Montreal Protocol, Geophysical Research Letters, 45, 401–409, https://doi.org/https://doi.org/10.1002/2017GL075345, 2018.

Pommrich, R., Müller, R., Grooß, J.-U., Konopka, P., Ploeger, F., Vogel, B., Tao, M., Hoppe, C. M., Günther, G., Spelten, N., Hoffmann, L., Pumphrey, H.-C., Viciani, S., D'Amato, F., Volk, C. M., Hoor, P., Schlager, H., and Riese, M.: Tropical troposphere to stratosphere transport of carbon monoxide and long-lived trace species in the Chemical Lagrangian Model of the Stratosphere (CLaMS), Geoscientific Model Development, 7, 2895–2916, https://doi.org/10.5194/gmd-7-2895-2014, 2014.

Prignon, M., Chabrillat, S., Friedrich, M., Smale, D., Strahan, S. E., Bernath, P. F., Chipperfield, M. P., Dhomse, S. S., Feng, W., Minganti, D., Servais, C., and Mahieu, E.: Stratospheric Fluorine as a Tracer of Circulation Changes: Comparison Between Infrared Remote-Sensing Observations and Simulations With Five Modern Reanalyses, Journal of Geophysical Research: Atmospheres, 126, e2021JD034 995, https://doi.org/https://doi.org/10.1029/2021JD034995, 2021.

Seidel, D. J., Fu, Q., Randel, W. J., and Reichler, T. J.: Widening of the tropical belt in a changing climate, Nature geoscience, 1, 21–24, https://doi.org/https://doi.org/10.1038/ngeo.2007.38, 2008.

Sheese, P. and Walker, K.: Data Quality Flags for ACE-FTS Level 2 Version 4.1/4.2 Data Set, https://doi.org/10.5683/SP2/BC4ATC, 2022.

Sheese, P. E., Boone, C. D., and Walker, K. A.: Detecting physically unrealistic outliers in ACE-FTS atmospheric measurements, Atmospheric Measurement Techniques, 8, 741–750, https://doi.org/10.5194/amt-8-741-2015, 2015.

Steiner, A. K., Ladstädter, F., Randel, W. J., Maycock, A. C., Fu, Q., Claud, C., Gleisner, H., Haimberger, L., Ho, S.-P., Keckhut, P., Leblanc, T., Mears, C., Polvani, L. M., Santer, B. D., Schmidt, T., Sofieva, V., Wing, R., and Zou, C.-Z.: Observed Temperature Changes in the Troposphere and Stratosphere from 1979 to 2018, Journal of Climate, 33, 8165 – 8194, https://doi.org/https://doi.org/10.1175/JCLI-D-19-0998.1, 2020.

Stiller, G. P., von Clarmann, T., Höpfner, M., Glatthor, N., Grabowski, U., Kellmann, S., Kleinert, A., Linden, A., Milz, M., Reddmann, T., Steck, T., Fischer, H., Funke, B., López-Puertas, M., and Engel, A.: Global distribution of mean age of stratospheric air from MIPAS SF_6 measurements, Atmospheric Chemistry and Physics, 8, 677–695, https://doi.org/10.5194/acp-8-677-2008, 2008.

https://doi.org/10.5194/egusphere-2024-1736
Preprint. Discussion started: 18 July 2024

Stiller, G. P., Fierli, F., Ploeger, F., Cagnazzo, C., Funke, B., Haenel, F. J., Reddmann, T., Riese, M., and von Clarmann, T.: Shift of subtropical transport barriers explains observed hemispheric asymmetry of decadal trends of age of air, Atmospheric Chemistry and Physics, 17, 11 177–11 192, https://doi.org/10.5194/acp-17-11177-2017, 2017.

Strahan, S. E., Smale, D., Douglass, A. R., Blumenstock, T., Hannigan, J. W., Hase, F., Jones, N. B., Mahieu, E., Notholt, J., Oman, L. D., Ortega, I., Palm, M., Prignon, M., Robinson, J., Schneider, M., Sussmann, R., and Velazco, V. A.: Observed Hemispheric Asymmetry in Stratospheric Transport Trends From 1994 to 2018, Geophysical Research Letters, 47, e2020GL088 567, https://doi.org/https://doi.org/10.1029/2020GL088567, 2020.

Vallis, G. K., Zurita-Gotor, P., Cairns, C., and Kidston, J.: Response of the large-scale structure of the atmosphere to global warming, Quarterly Journal of the Royal Meteorological Society, 141, 1479–1501, https://doi.org/https://doi.org/10.1002/qj.2456, 2015.

Wallace, J. M., Panetta, R. L., and Estberg, J.: Representation of the Equatorial Stratospheric Quasi-Biennial Oscillation in EOF Phase Space, Journal of Atmospheric Sciences, 50, 1751–1762, https://doi.org/https://doi.org/10.1175/1520-0469(1993)050<1751:ROTESQ>2.0.CO;2, 1993.

Waugh, D. and Hall, T.: Age of stratospheric air: theory, observations, and models, Reviews of Geophysics, 40, 1–1–1–26, https://doi.org/https://doi.org/10.1029/2000RG000101, 2002.